

Article

Noise Immunity Analysis and Improvement of dq Frame Based Open-Loop Phase Detection Scheme

Xiaobo Li ^{1,*}, Mingxian Li ^{1,*}, Hua Chai ² and Binbing Wu ³

¹ School of Electrical and Power Engineering, China University of Mining and Technology, Xuzhou 221116, China

² Department of Electrical Engineering, Shanxi University, Taiyuan 030013, China; 332326637@foxmail.com

³ School of Electrical Engineering, Xinjiang University, Wulumuqi 830049, China; 254849448@foxmail.com

* Correspondence: xbli_cumt@126.com (X.L.); mingxian.li@foxmail.com (M.L.); Tel.: +86-1381-442-5655 (X.L.)

Received: 14 February 2020; Accepted: 2 March 2020; Published: 3 March 2020



Abstract: To improve the noise immunity of a dq frame based open-loop phase detection (OPD) under high-frequency noise grid conditions, this paper develops a detailed model to quantitatively evaluate the phase detection error and noise immunity. It is found that the OPD behaves differently in terms of noise immunity when the dq frame is in different angle positions with the grid voltage. When the grid voltage coincides with the d axis, the high-frequency noise has the smallest impact on the phase detection accuracy, and the OPD thus has the strongest noise immunity. Inspired by this conclusion, an improved OPD algorithm is proposed in this paper, which can effectively reduce the phase detection error by fine-tuning the rotation angle of the dq frame to ensure that the angle between the voltage vector and d axis is always close to 0. The improved OPD algorithm has a fast and precise character to detect the phase information with less error and is flexible for application. Under heavy noise grid conditions, it can also effectively shorten the dynamic response time in the phase-detecting process using a low-pass filter (LPF) with a higher cut-off frequency. The correctness of the noise immunity analysis and the effectiveness of the improved OPD algorithm are verified by the simulations and experimental results in MATLAB and RT-LAB.

Keywords: noise immunity; open-loop phase detection (OPD); voltage phase; coordinate transformation

1. Introduction

The voltage synchronous phase is one of the key signals of converter control systems in distributed power generation systems. It is of paramount importance to detect the voltage phase quickly and accurately for high-performance system control strategies [1,2]. In recent years, increasing numbers of power electronic devices have been put into operation for electricity transformation in the power system. However, the collected power voltage signal often contains high-frequency random noise, which greatly interferes with the accurate detection of the voltage phase and becomes an unfavorable factor for achieving the high-performance control of grid-connected inverters [3–5]. Thus, phase detection schemes should have excellent noise immunity to suppress the interference.

In practical terms, phase detection schemes can be divided into open-loop phase detection (OPD) and closed-loop phase detection (CPD). The open-loop phase detection scheme eliminates the PI adjustment process, which can realize the rapid detection of the voltage phase. It is always applied to conditions such as a relatively ideal grid environment, and the requirement of phase accuracy is not very high [6–8]. A zero-crossing phase detection scheme is suggested in [8], which is the most commonly used OPD scheme at present. Its basic principle is to take the zero-crossing point as the reference point, and then the grid voltage phase can be calculated at each moment. However, high-frequency noise will affect the accurate detection of the zero-crossing point and result in phase

detection errors. An OPD scheme based on the dq frame is given in [9], which focuses on the phase detection of single-phase voltage. In [9], a voltage signal is substituted into the rotational dq frame and converted into the voltage DC component. Then, the single-phase voltage can be quickly determined by a simple calculation. However, it is observed that noise will cause a DC component error after abc/dq transformation, which will thus result in a phase error. Moreover, at least two-phase orthogonal signals are required to complete the coordinate transformation. Delaying the sampling period to construct an orthogonal signal will result in high-frequency noise amplification, which thus further causes phase steady-state error [4]. In [10], the authors focus on the rapid phase detection of unbalanced grid voltage, which significantly improves the phase detection speed under complex conditions. However, while extracting the voltage-positive sequence components, random noise may still be amplified during the construction of the orthogonal voltage signal by delaying the sampling period or the first-order differentiating method [11].

An OPD based on the dq frame scheme has advantages in terms of obtaining the real-time voltage phase and dealing with frequency step changes or phase jumps, and it can realize the fast detection of voltage phases and ensure the superiority of a grid-tied converter control system under adverse grid conditions. However, high-frequency noise is a factor which cannot be ignored and will cause fluctuation changes in the voltage current magnitude and thus result in phase detection errors. A low-pass filter (LPF) is introduced as an effective solution to attenuate high-frequency random noise [9–12]. Reducing the filter bandwidth can effectively suppress noise; however, it will limit the dynamic performance of the control system at the same time, which leads to a longer system dynamic response time.

Noise immunity is a key part in the higher phase accuracy of an open-loop phase detection scheme based on a dq frame. Therefore, it is very important not only to study the influencing factors of noise immunity in detail but also to effectively suppress high-frequency noise to reduce phase error and simultaneously ensure the rapidity of phase detection methods.

The paper is organized as follows. Section 2 presents the basic principle of the dq frame-based OPD scheme suggested in [9,10]. Section 3 establishes a detailed phase error analysis model to evaluate the noise immunity of OPD. The improved OPD algorithm achieved by fine-tuning the rotation angle of the dq frame is presented in Section 4. MATLAB/RT-LAB simulation studies for the enhanced algorithm are presented in Section 5. Conclusions are given in Section 6.

2. Basic Principles of OPD

First, three-phase balanced voltages can be described by

$$\begin{bmatrix} U_a \\ U_b \\ U_c \end{bmatrix} = \begin{bmatrix} U_m \sin(\omega t + \theta) \\ U_m \sin(\omega t - 2\pi/3 + \theta) \\ U_m \sin(\omega t + 2\pi/3 + \theta) \end{bmatrix} \quad (1)$$

where U_m , ω and θ represent the voltage magnitude, the grid frequency and initial phase, respectively.

Using Clarke's and Park's transformation, the voltages $\mathbf{U} = [U_a \ U_b \ U_c]^T$ in Equation (1) are transformed as U_d and U_q as follows:

$$\begin{bmatrix} U_d \\ U_q \end{bmatrix} = T_{abc/dq}(\omega t) \begin{bmatrix} U_a \\ U_b \\ U_c \end{bmatrix} = \frac{2}{3} \begin{bmatrix} \sin \omega t & \sin(\omega t - 2\pi/3) & \sin(\omega t + 2\pi/3) \\ \cos \omega t & \cos(\omega t - 2\pi/3) & \cos(\omega t + 2\pi/3) \end{bmatrix} \begin{bmatrix} U_a \\ U_b \\ U_c \end{bmatrix} \quad (2)$$

The DC components of the three-phase voltages can thus be expressed as

$$\begin{cases} U_d = U_m \cos \theta \\ U_q = U_m \sin \theta \end{cases} \quad (3)$$

From Figure 1, it can be seen that the initial phase θ of the three-phase grid voltages is the angle between \mathbf{U} and the d axis.

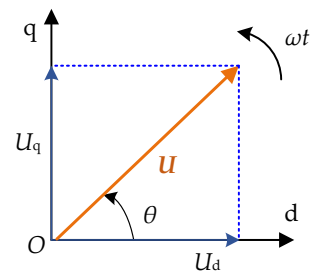


Figure 1. Voltage vector diagram in the dq frame.

The voltage initial phase θ can thus be captured by

$$\theta = \arctan\left(\frac{U_q}{U_d}\right) \quad (4)$$

We define the initial phase angle as agreeing with $[0, 2\pi)$; however, the phase computed by Equation (4) belongs to $(-\pi/2, \pi/2)$. To convert the initial angles to the set interval, this paper employs a compensation phase θ_{ex} , which is defined by

$$\theta_{ex} = \begin{cases} 0 & U_d > 0, U_q > 0 \\ 0 & U_q = 0 \\ 0 & U_d = 0, U_q > 0 \\ \pi & U_d < 0, U_q \neq 0 \\ \pi & U_d = 0, U_q < 0 \\ 2\pi & U_d > 0, U_q < 0 \end{cases} \quad (5)$$

In summary, the current position of the three-phase voltages can thus be computed as

$$\varphi = \omega t + \theta = \omega t + \arctan\left(\frac{U_q}{U_d}\right) + \theta_{ex} \quad (6)$$

Similarly, the magnitude of grid voltages also can be computed as

$$U_m = \sqrt{(U_q)^2 + (U_d)^2} \quad (7)$$

For the ideal grid voltage conditions without high-frequency random noise interference, substitute Equation (1) into Equations (2), (5) and (7); the instantaneous magnitude and synchronous phase can be captured immediately and accurately, respectively.

However, when noise interference occurs, the computed magnitude of the grid voltages undoubtedly contains random fluctuations. As shown in Figure 2, the actual detection phase computed by Equation (4) thus offsets the actual value, which results in an obvious phase error.

In brief, the OPD based on the dq frame exhibits the advantages of rapidity and simplicity, which can detect voltage synchronous phase faster than traditional CPDs and thus ensure the high-performance operation of grid-connected inverters. It is worth noticing that the important premise of improving phase measurement accuracy is to ensure the rapidity of the OPD scheme under noise conditions. Based on this premise, it is necessary to evaluate the noise immunity and thus propose an enhanced scheme to ensure that the phase error is acceptable.

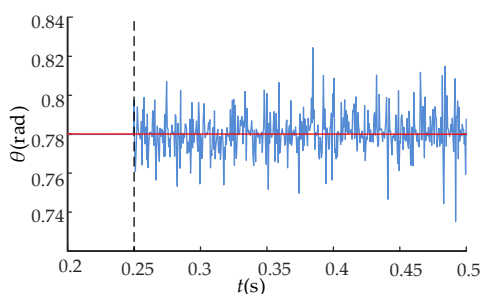


Figure 2. Initial phase waveform under high-frequency random noise conditions.

3. Noise Immunity Analysis Model of OPD

The grid voltages are regarded as the combination of the three-phase balanced grid voltages and the high-frequency noise DC components. Thus, the three-phase voltage signal with high-frequency noise could be described as

$$\tilde{U} = [\tilde{U}_a \quad \tilde{U}_b \quad \tilde{U}_c]^T \tag{8}$$

The physical quantities with superscript \sim in this paper indicate the existence of random noise. Considering the existence of high-frequency random noise, Equation (4) can be rewritten as

$$Y = \tan\theta^* = \frac{\tilde{U}_q}{\tilde{U}_d} = \frac{U_q \pm x_q}{U_d \pm x_d} = \frac{\sin\theta \pm \frac{x_q}{U_m}}{\cos\theta \pm \frac{x_d}{U_m}} \tag{9}$$

In Equation (9), x_q and x_d denote noise values in the dq frame, respectively. θ^* is the actual detection phase. Assume $x_q \leq N$, $x_d \leq N$, where N is the possible maximum noise value; to analyze the noise immunity systematically in this paper, we define λ as the noise ratio of grid voltages, which can be expressed as

$$\lambda = \frac{N}{U_m} > 0 \tag{10}$$

By incorporating Equations (9) and (10), we can get

$$\begin{cases} \sin\theta + x_q/U_m \leq \sin\theta + \lambda \\ \cos\theta + x_d/U_m \leq \cos\theta + \lambda \\ \sin\theta - x_q/U_m \geq \sin\theta - \lambda \\ \cos\theta - x_d/U_m \geq \cos\theta - \lambda \end{cases} \tag{11}$$

Figure 3 shows that if the initial phase interval is $\theta \in (0, \pi/2)$, obviously, $\sin\theta > 0$ and $\cos\theta > 0$. In the case of $\cos\theta - \lambda = 0$ or $\sin\theta - \lambda = 0$, we can observe that $\theta = \arccos\lambda$ or $\theta = \arcsin\lambda$, respectively.

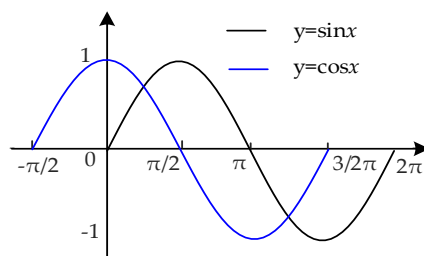


Figure 3. Partial waveforms of sine and cosine functions when $\theta \in (0, \pi/2)$.

First, we divide the initial phase interval $(0, \pi/2)$ into three intervals (i.e., $\theta \in (0, \arcsin\lambda)$, $(\arcsin\lambda, \arccos\lambda)$, and $(\arccos\lambda, \pi/2)$). Next, to evaluate the noise immunity of different initial phases in the dq frame, this paper deduces the error formula of these three intervals, respectively.

In the case of θ ($\arcsin \lambda$, $\arccos \lambda$), it is notable that $\sin \theta \pm \lambda > 0$ and $\cos \theta \pm \lambda > 0$; as shown in Figure 4, the initial phase calculated by Equation (9) satisfies

$$\theta_{\min} \leq \theta^* \leq \theta_{\max} \tag{12}$$

where

$$\theta_{\max} = \arctan\left(\frac{\sin \theta + \lambda}{\cos \theta - \lambda}\right) \tag{13}$$

$$\theta_{\min} = \arctan\left(\frac{\sin \theta - \lambda}{\cos \theta + \lambda}\right) \tag{14}$$

As displayed in Figure 4, the maximum phase error can thus be denoted as

$$\Delta\theta_{\max} = \max\{\Delta\theta|_{\text{Upper}}, \Delta\theta|_{\text{Lower}}\} \tag{15}$$

In Equation (15),

$$\Delta\theta|_{\text{Upper}} = \theta_{\max} - \theta = \arctan\left(\frac{\sin \theta + \lambda}{\cos \theta - \lambda}\right) - \theta \tag{16}$$

$$\Delta\theta|_{\text{Lower}} = \theta - \theta_{\min} = \theta - \arctan\left(\frac{\sin \theta - \lambda}{\cos \theta + \lambda}\right) \tag{17}$$

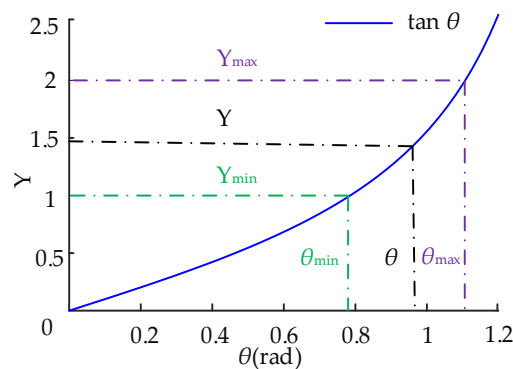


Figure 4. The calculation error analysis of voltages phase under random noise interference.

Figure 5 compares the phase error deduced in Equations (16) and (17). We can see that if $\theta \in (\arcsin \lambda, \pi/4)$, the maximum phase error $\Delta\theta_{\max}$ equals $\Delta\theta|_{\text{Upper}} = \theta_{\max} - \theta$. Thus, the value of the actual detection θ^* deviates upwards from the theoretical value.

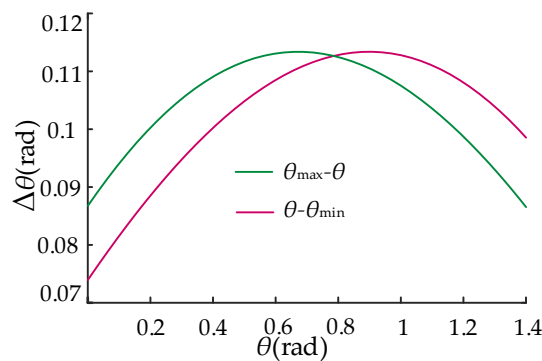


Figure 5. The relationship of $\Delta\theta$ to the initial phase θ when $\theta \in (\arcsin \lambda, \arccos \lambda)$.

In the case of $\theta \in (\pi/4, \arccos \lambda)$, we can see that $\Delta\theta_{\max}$ equals $\Delta\theta|_{\text{Lower}} = \theta - \theta_{\min}$; i.e., the actual detection value falls away from the theoretical value.

In the case of $\theta \in (0, \arcsin \lambda)$, from Equation (11), it is easy to observe that $\theta_{\min} < 0$, $\theta_{\max} > 0$, and $|\theta_{\min}| < \theta_{\max}$. Thus, the maximum phase error in the interval can be expressed as

$$\Delta\theta_{\max} = \arctan\left(\frac{\sin \theta + \lambda}{\cos \theta - \lambda}\right) - \theta, \theta \in (0, \arcsin \lambda) \quad (18)$$

When $\theta \in (\arccos \lambda, \pi/2)$, we can see that $\theta_{\max} < 0$, $\theta_{\min} > 0$, and $\theta_{\min} < |\theta_{\max}|$. From Equation (6), if $\theta < 0$, the compensation phase θ_{ex} equals π . Thus, the maximum phase error can be obtained as

$$\Delta\theta_{\max} = \arctan\left(\frac{\sin \theta + \lambda}{\cos \theta - \lambda}\right) + \pi - \theta, \theta \in \left(\arccos \lambda, \frac{\pi}{2}\right) \quad (19)$$

As aforementioned, in the case of $\theta \in (0, \pi/2)$, the expression of $\Delta\theta_{\max}$ corresponding to different initial phases under noise conditions can be expressed as

$$f(\theta)_{\max} = \begin{cases} \arctan\left(\frac{\sin \theta + \lambda}{\cos \theta - \lambda}\right) - \theta, \theta \in [0, \frac{\pi}{4}) \\ \theta - \arctan\left(\frac{\sin \theta - \lambda}{\cos \theta + \lambda}\right), \theta \in (\frac{\pi}{4}, \arccos \lambda) \\ \arctan\left(\frac{\sin \theta + \lambda}{\cos \theta - \lambda}\right) + \pi - \theta, \theta \in (\arccos \lambda, \frac{\pi}{2}) \end{cases} \quad (20)$$

According to Figure 1 and Equation (20), we can see that the initial phase is the angle between the voltage vector \mathbf{U} and d axis. Obviously, a different initial phase means that if the dq frame is in different positions with voltage \mathbf{U} , this will thus lead to a different voltage initial phase error under high-frequency random noise interference.

In Equation (20), the maximum phase error of $\theta \in (0, \pi/4)$ and $(\pi/4, \arccos \lambda)$ could, respectively, be obtained by

$$\begin{cases} \theta_1 = \frac{\pi}{4} - \arcsin(\sqrt{2}\lambda) \approx \frac{\pi}{4} \\ \theta_2 = \frac{\pi}{4} + \arcsin(\sqrt{2}\lambda) \approx \frac{\pi}{4} \end{cases} \quad (21)$$

From Equation (21), it can be observed that, when the angle between \mathbf{U} and d axis is around 45° , the phase error is the largest and the noise immunity of OPD is the worst. The maximum phase error is shown as

$$f\left(\frac{\pi}{4}\right) = \arcsin(\sqrt{2}\lambda) \quad (22)$$

In addition, substituting $\theta = 0$, $\theta_3 = \arcsin \lambda$, $\theta_4 = \arccos \lambda$ into Equation (20), it is easy to observe that

$$f(\theta_4) > f(\theta_3) > f(0) = \arctan\left(\frac{\lambda}{1-\lambda}\right) \approx \lambda \quad (23)$$

From Equation (23), it can be seen that, if the angle between \mathbf{U} and d axis is 0° , high-frequency noise has the weakest interference on the phase measurement accuracy, and the phase error is thus the smallest.

In the case of the initial phase belonging to the other quadrants, the analysis process and scheme are the same as above and will not be repeated in this paper.

In the actual operating condition, assume that the phase measurement accuracy of the grid-tied inverter is K under noise interference. From Equation (22), the maximum phase error can be expressed as

$$\frac{\Delta\theta_{\max}}{2\pi} = \frac{\arcsin(\sqrt{2}\lambda)}{2\pi} < K \quad (24)$$

From Equation (24), the relationship between the phase-precision K and noise ratio λ can be expressed as

$$K > \frac{\sqrt{2}}{2\pi}\lambda \approx 0.2251\lambda \quad (25)$$

If the voltage phase-accuracy is set as $K < 2\%$, the accepted range of the voltage noise ratio agrees with $0 < \lambda < 8.88\%$. This means that, if the original voltage magnitude is 100 V and the noise signal value does not exceed 8.88 V, the phase error detected by OPD can meet the accuracy requirement. However, when the high-frequency random noise increases, the phase error is thus larger, which does not meet the requirement of practical accuracy.

From Figure 6, if the noise ratio agrees with $0 < \lambda < 0.1$, the initial phase fluctuates at about 45° , which corresponds to the maximum phase error. However, when λ increases, as shown in Figure 6 and Equation (21), θ_1 and θ_2 are not at the maximum value point.

The bigger λ is, the more θ_1 and (or) θ_2 deviate from $\pi/4$, which will lead to the amplification of $\Delta\theta_{\max}$ and other phase errors.

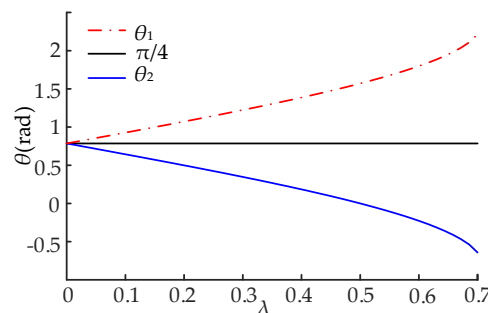


Figure 6. The relation of the noise ratio to the voltage initial phase, which results in the maximum phase error.

In summary, the conclusions of noise immunity on OPD are as follows:

- The voltage initial phase detection error is associated with the voltage noise ratio λ . The greater the voltage noise ratio, the greater the phase error. The accuracy of phase detection is greatly affected by the noise value.
- If the angle between \mathbf{U} and d axis is different, OPD has a different noise immunity. When $\theta \approx 45^\circ$, the phase error is the largest. If $\theta = 0^\circ$, the phase error is the smallest, and the noise interference to phase accuracy is the lowest.

4. Improved OPD

Based on the above, to reduce the phase error, this paper proposes an improved OPD to enhance the noise immunity of OPD. First, the rotation angle of the dq frame is fine-tuned to ensure that the angle between the voltage vector and d axis is always close to 0° , so that the voltage vector could be located in the angle position with the smallest phase error in the dq frame. The noise immunity of OPD could thus be enhanced, and the initial phase detection accuracy can thus be improved. The enhanced OPD algorithm is elaborated in detail below.

From Equation (2) and Figure 1, it can be seen that, in Clarke's and Park's transformation, ωt is the rotation angle of the dq frame, which determines the rotation speed and relative position relationship between the dq frame and voltage vector \mathbf{U} . For a different initial phase θ and fixed frequency, the actual detected phase value θ^* has a different phase error (i.e., the closer θ is to $\pi/4$, the larger the detected phase error). Hence, $\omega t + \theta$ can be used as a simple and effective controlled factor to fine-tune the position of the dq frame.

As shown in Figure 7, θ^* is the actual detected value of the voltage initial phase under noise interference. θ_{d0} is the difference between the theoretical initial phase and actual detected value; i.e., the angle between the d_0 axis and voltage \mathbf{U} .

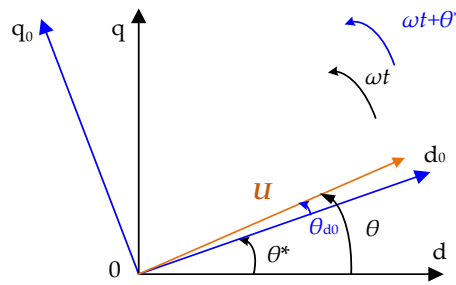


Figure 7. The diagram of the fine-tuning of the rotation angle of dq frame.

When adding the detected phase value θ^* to the dq coordinate transformation matrix to fine-tune the dq frame, $T_{abc/dq}(\omega t + \theta^*)$ can thus be rewritten as

$$T_{abc/dq}(\omega t + \theta^*) = \frac{2}{3} \begin{bmatrix} \sin(\omega t + \theta^*) & \sin(\omega t + \theta^* - 2\pi/3) & \sin(\omega t + \theta^* + 2\pi/3) \\ \cos(\omega t + \theta^*) & \cos(\omega t + \theta^* - 2\pi/3) & \cos(\omega t + \theta^* + 2\pi/3) \end{bmatrix} \quad (26)$$

After fine-tuning the rotation angle of the dq frame, the voltage DC components in the d_0q_0 frame can thus be expressed as follows:

$$\begin{cases} U_{d0} = U_m \cos(\theta - \theta^*) \\ U_{q0} = U_m \sin(\theta - \theta^*) \end{cases} \quad (27)$$

From Equation (27), the current position of the three-phase voltages could be calculated by

$$\varphi = \omega t + \theta^* + \arctan\left(\frac{U_{q0}}{U_{d0}}\right) + \theta_{ex} \quad (28)$$

From Equation (28), it can be observed that, under the ideal grid environment (i.e., $\theta^* = \theta$), the current position of the three-phase voltages calculated by Equation (28) equals that of Equation (6), which shows that the improved OPD algorithm has the same phase detection function as the original OPD.

When the three-phase voltages contain high-frequency random noise, we take $\theta = \pi/4$ as an example to better illustrate the effect of fine-tuning the rotation angle dq frame to reduce phase detection errors.

First, the relationship between θ^* and θ_{d0} can be expressed as

$$\theta_{d0} = \theta - \theta^* = \arctan\left(\frac{U_{q0}}{U_{d0}}\right) + \theta_{ex} \quad (29)$$

From Equation (22), we can see that if θ equals $\pi/4$, the phase error $\Delta\theta$ (i.e., θ_{d0}) equals $\arcsin(\lambda^{1/2})$ and the actual detected value θ^* equals $\pi/4 - \arcsin(\lambda^{1/2})$; using the original OPD, the current position of the three-phase voltages in the dq frame is shown as

$$\varphi_{dq} = \omega t + \frac{\pi}{4} - \arcsin(\sqrt{2}\lambda) \quad (30)$$

Using Equation (26) to fine-tune the dq frame, the DC components can thus be expressed as

$$\begin{cases} U_{d0}(\pi/4) = U_m \cos[\arcsin(\sqrt{2}\lambda)] \\ U_{q0}(\pi/4) = U_m \sqrt{2}\lambda \end{cases} \quad (31)$$

From Equation (31), the current position of the three-phase voltages in the d_0q_0 frame is shown as

$$\varphi_{d_0q_0} = \omega t + \frac{\pi}{4} - \arcsin(\sqrt{2}\lambda) + \frac{\sqrt{2}\lambda}{\cos[\arcsin(\sqrt{2}\lambda)]} \quad (32)$$

From Equations (30) and (32), it can be seen that $\varphi_{d_0q_0}$ in Equation (32) is closer to $\pi/4$ than φ_{dq} in Equation (30), which shows that the improved OPD algorithm can effectively reduce the phase detection error by fine-tuning the rotation angle of the dq frame.

Moreover, the phase error percentage comparison from Equations (30) and (32) is shown in Figure 8. It can be seen that the proposed improved OPD algorithm can significantly reduce the phase detection error and ensure that the phase detection error is acceptable.

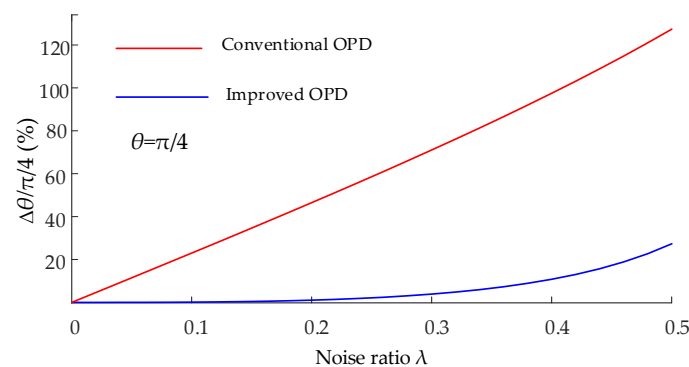


Figure 8. The comparison of the phase detection error with different open-loop phase detection methods (OPDs).

From Equation (32) and Figure 7, we can see that the larger θ_{d_0} , the larger the error calculated by Equation (31) in the d_0q_0 frame. While directly adding the initial phase detection value θ^* into the coordinate transformation matrix without considering the real-time variation of random noise value, which may result in a relatively large angle difference between the d_0 axis and voltage vector \mathbf{U} , the phase detection accuracy of the proposed OPD algorithm will thus be reduced.

Hence, it is of paramount importance to detect the value of θ_{d_0} in real time to further reduce the phase detection errors. To ensure that the grid voltage vector almost coincides with the d_0 axis in the d_0q_0 frame, the flow chart of tracking the θ_{d_0} between the voltage vector and d_0 axis and fine-tuning the relative angular position of d_0q_0 frame is shown in Figure 9.

The judgment condition of angle difference θ_{d_0} (i.e., $\arctan(U_{q_0}/U_{d_0}) + \theta_{ex}$) is set as follows:

- (1) After fine-tuning the rotation angle of the dq frame first, if $|\arctan(U_{q_0}/U_{d_0}) + \theta_{ex}| \leq 2\pi K$, it can be seen from Equation (24) that the voltage synchronous phase angle calculated by Equation (30) meets the phase accuracy requirements.
- (2) Conversely, while the judgment condition is not satisfied (i.e., $|\arctan(U_{q_0}/U_{d_0}) + \theta_{ex}| > 2\pi K$), the d_0q_0 frame must be fine-tuned again; $\arctan(U_{q_0}/U_{d_0}) + \theta_{ex}$ is simultaneously added to the dq coordinate transformation matrix in Equation (26) for the fine-tuning of the dq frame.

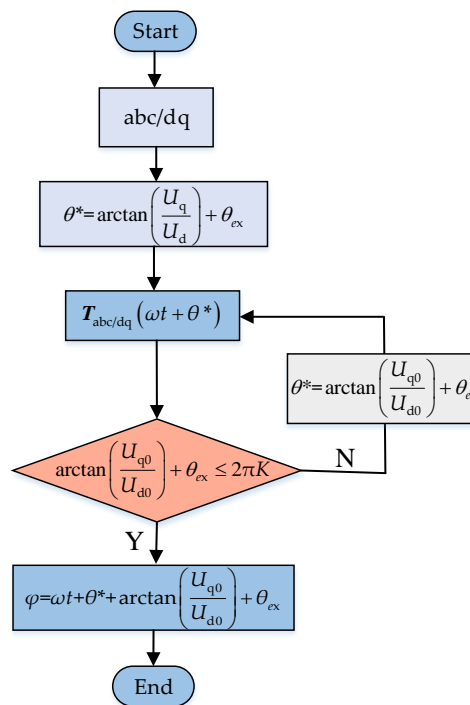


Figure 9. The flow chart of tracking the θ_{d0} and fine-tuning the angular position of the d_0q_0 frame.

Particularly, when the voltage phase detection requirement for engineering application is higher, even if the included angle of the d axis and voltage vector is close to 0, the phase error may not meet accuracy requirements. Although the enhanced OPD algorithm proposed in this paper can significantly suppress the interference of high-frequency random noise without using LPF, it is difficult to eliminate its influence completely (i.e., 100 % noise suppression).

To further attenuate noise, the high-frequency random noise can be filtered by LPF, however, which will simultaneously sacrifice the dynamic response performance of the control system. The improved OPD algorithm proposed in this paper has achieved the suppression of high-frequency noise for phase measurement accuracy, and the dynamic performance of OPD can thus be enhanced using an LPF with a higher cutoff frequency. The transfer function of the first-order LPF is given as

$$LPF(s) = \frac{\omega_f}{s + \omega_f} \tag{33}$$

where ω_f represents the cut-off frequency of LPF.

The scheme of the enhanced OPD algorithm adopting the improved algorithm proposed in this paper is shown in Figure 10.

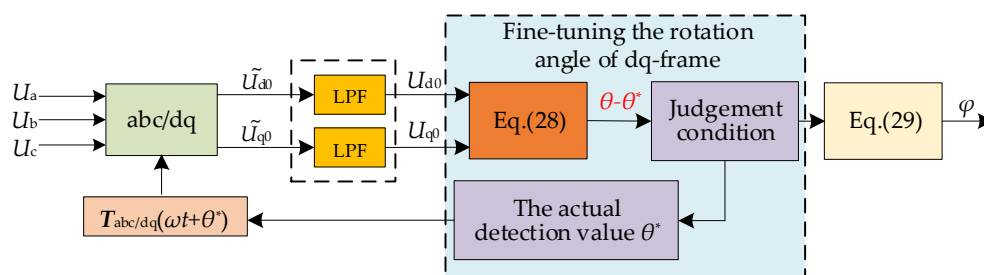


Figure 10. Scheme of the enhanced OPD by fine-tuning the rotation angle of the dq frame.

5. Simulation Verification

To evaluate the correctness of the noise immunity analysis on the OPD scheme and the enhanced algorithm, this paper implements OPD verification based on MATLAB/Simulink and RT-LAB.

The purpose of verification is to prove that the enhanced algorithm is effective at improving the phase measurement accuracy under different working conditions, such as by adding noise suddenly, frequency step change, increasing the noise ratio λ and θ , and through comparison with the addition of LPF, where $U_m = 100$ V in the simulation scenario.

The three-phase voltage parameters of simulation verification are shown in Table 1:

Table 1. Voltage parameters under different condition.

Signal Parameters	$\theta(\text{rad})$	$f(\text{Hz})$	λ
Normal condition	$\pi/4$	50	0
Adding noise	$\pi/4$	50	0.1
Frequency step change	$\pi/4$	55	0.1
Increased λ	$\pi/4$	50	0.2
Increased θ	0	50	0.2

5.1. Noise Immunity Verification of OPD

Figure 11 shows that when high-frequency noise is suddenly added to a grid voltage at 0.5 s, the current magnitude of the grid voltage fluctuates, and the current position waveform captured by conventional OPD thus greatly deviates. The error of phase detection increases, which will count against the high-performance control of the grid-connected inverter.

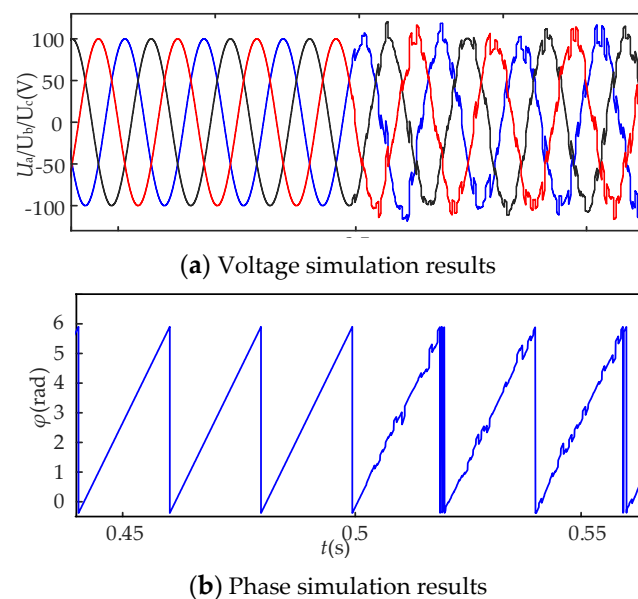


Figure 11. Three-phase voltage and phase simulation waveform captured by the conventional OPD.

For the different initial phase θ under high-frequency noise interference (i.e., the angle between \mathbf{U} and d axis is different), the phase simulation results detected by the conventional OPD are shown in Figure 12. It can be observed that, when the initial phase of grid voltage is 45° , the noise has the largest interference on the initial phase measurement; the noise immunity is the worst, and the voltage phase error is the largest. When the angle between the voltage vector and d axis is close to 0, the phase error is the smallest. The experimental results are consistent with the above analysis.

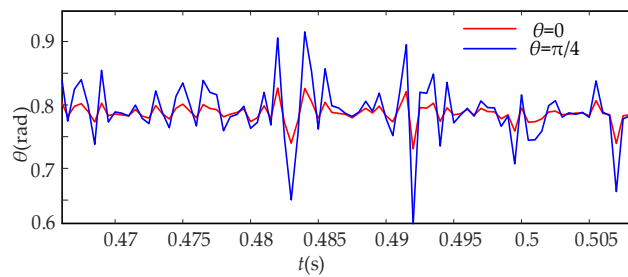


Figure 12. The different initial phase simulation waveforms.

Figure 13 shows the phase measurement waveform comparison results when the power grid frequency changes from 50 Hz to 55 Hz. The initial phase waveform detected by the improved algorithm presented in this paper hardly changes under the condition of frequency step change, which could imply that the voltage initial angle detected by this improved algorithm is almost unaffected.

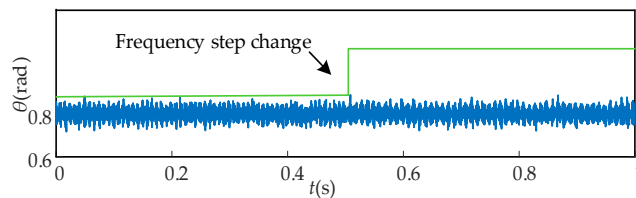


Figure 13. Phase simulation with the improved algorithm during frequency step change.

Figure 14 shows the initial phase response waveform contrast when the noise ratio changes from 0.1 to 0.2. The result shows that as the voltage noise ratio increases, the interference degree to voltage noise immunity becomes larger, and the phase error increases significantly.

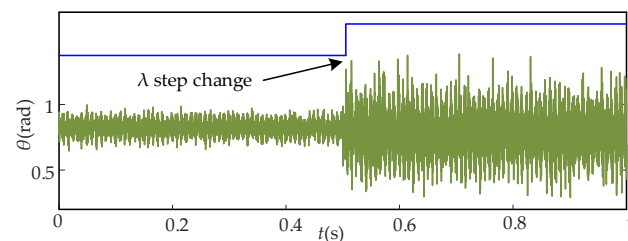


Figure 14. Initial phase response waveform with increased noise ratio.

Figure 15 shows the initial phase waveform response process using the improved algorithm. The waveform shows that by fine-tuning the rotation angle of the dq frame, the phase error of voltage initial phase is significantly smaller than that of the conventional OPD, and the phase error is almost equal to $\theta = 0^\circ$. The phase error mainly depends on the magnitude of the voltage signal–noise ratio. The proposed algorithm can improve the phase measurement accuracy under noise interference.

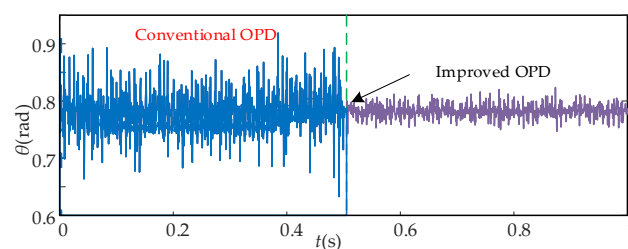


Figure 15. Initial phase simulation results when adopting the improved algorithm.

In Figure 16, the green phase waveform is captured by the conventional OPD when the phase angle increases from 0 to $\pi/4$. The blue one is captured by the improved OPD.

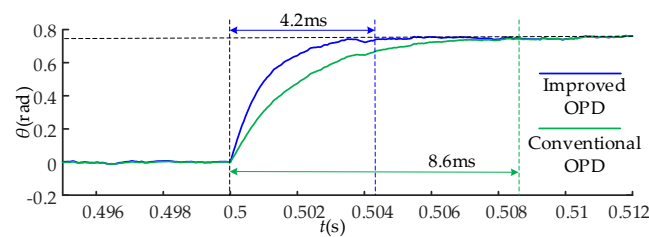


Figure 16. Response time comparison with different OPDs.

To get the same random noise suppression effect, the conventional OPD sets ω_f as 1 kHz, while the improved OPD sets ω_f as 5 kHz. From Figure 15, it can be seen that the improved OPD algorithm effectively avoids noise amplification, and the ω_f can therefore be higher (i.e., 5 kHz), which is conducive to shortening the response time (about 4.2 ms). However, to obtain a better noise attenuation effect, the conventional OPD is set ω_f as 1 kHz, which thus results in the poor dynamic performance of the phase detection process; its response time is about 8.6 ms.

5.2. Real-Time Simulation Experiment Verification

In this paper, after using MATLAB/Simulink to build the analysis model of OPD and its enhanced algorithm, a real-time simulation platform based on RT-LAB is imported for comparative verification.

In the experimental scenario, the voltage phase changes suddenly, as shown in Figure 17a. The DC component results detected by the conventional OPD are shown in Figure 17b,c, respectively.

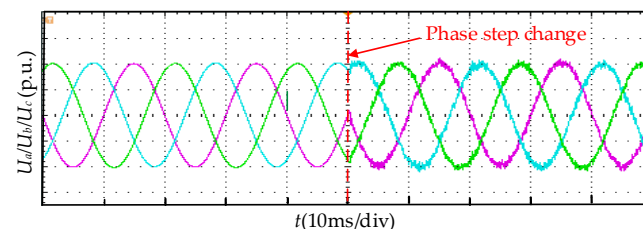
As shown in Figure 17d,e, the response time of the improved OPD is shorter than the conventional OPD when the phase changes from 0 to $\pi/4$; the conventional OPD sets ω_f as 2 kHz and the improved OPD sets ω_f as 6 kHz. According to the experimental result, under the same noise suppression effect, the improved OPD makes the response process faster, which is important to achieving the high-performance control of grid-connected inverters. It can be noticed that the effectiveness of the improved OPD algorithm has also been verified by RT-LAB.

To demonstrate the technical advantages of the improved OPD algorithm in terms of the dynamic response speed and digital implementation, this paper compares its dynamic response time with the widely used SSRF-SPLL and DDSRF-SPLL algorithms. The experimental conditions and comparative analysis results are shown in Table 2.

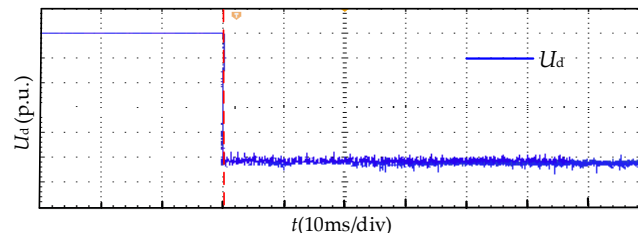
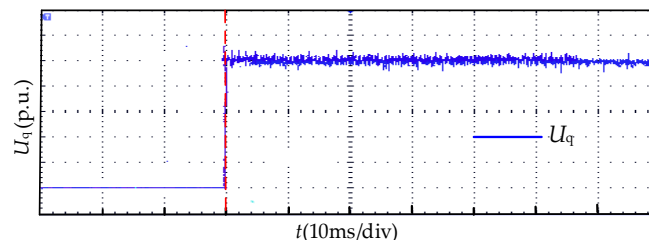
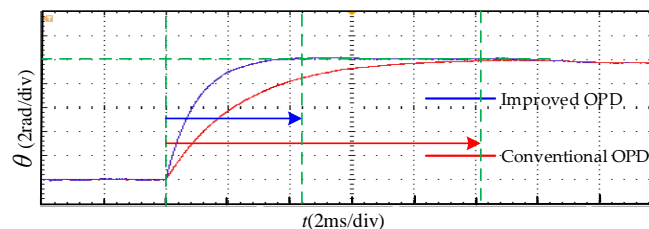
Table 2. Comparison result of dynamic response time (ms).

Algorithms	Amplitude Change	Wave Distortion	Phase Change + $\lambda = 0.08$	Phase Change + $\lambda = 0.2$	Frequency Drop
SSRF-SPLL	<0.5	<0.5	<4	<10	<15
DDSRF-SPLL	<0.5	<0.5	<4	<10	<35
Proposed OPD	<0.5	<0.5	<2 (no LPF)	<5 (with LPF)	<15

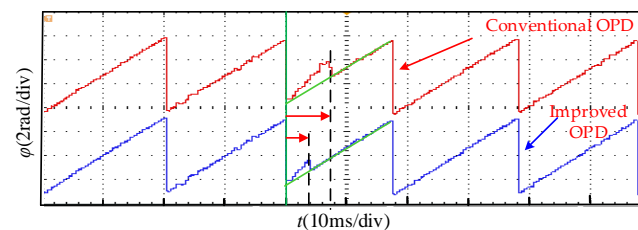
It can be seen in Table 2 that, under the experimental conditions of amplitude change and waveform distortion, all three phase detection algorithms have a fast dynamic response speed. When the impact of high-frequency random noise is small (i.e., $\lambda = 0.08$), the proposed OPD can respond quicker to the dynamic processes without using LPF. When $\lambda = 0.2$, the dynamic response time of the three methods increased to varying degrees. However, the proposed OPD still responds quicker using an LPF with a lower cut-off frequency. To obtain better noise suppression, the other two algorithms significantly sacrifice dynamic performance.



(a) Three-phase voltage

(b) DC voltage component U_d (c) DC voltage component U_q 

(d) Initial phase comparison results



(e) Synchronous phase comparison results

Figure 17. Experimental results.

6. Conclusions

The fast and accurate acquisition of a grid voltage synchronous phase is the basic requirement of the high-performance control of grid-connected inverters. This paper focuses on the noise immunity of OPD and proposes a novel, enhanced OPD algorithm to improve the phase accuracy without sacrificing response time. Based on the theoretical analysis and simulation results, our conclusions are as follows:

- (1) If the included angle between the voltage vector and d axis is about 45° , the phase measurement accuracy is most affected by noise. When the included angle equals 0, the noise immunity is the strongest and the phase error is the smallest. The voltage phase error depends on the noise ratio.
- (2) By fine-tuning the rotation angle of the dq frame, which can ensure that the voltage U is always at the position with minimum noise interference in the dq frame and enhance the noise immunity of OPD, the phase error can thus be ensured to be acceptable.

Author Contributions: Conceptualization, X.L. and M.L.; Methodology, M.L.; Software, M.L.; Validation, M.L.; Formal Analysis, H.C.; Investigation, B.W.; Resources, M.L.; Data Curation, M.L.; Writing—Original Draft Preparation, M.L.; Writing—Review & Editing, M.L.; Visualization, M.L.; Supervision, M.L.; Project Administration, M.L. All authors have read and agreed to the published version of the manuscript.

Funding: This research received no external funding.

Conflicts of Interest: The authors declare no conflict of interest.

References

1. Singh, B. Implementation of single-phase enhanced phase-locked loop-based control algorithm for three-phase DSTATCOM. *IEEE Trans. Power Deliv.* **2013**, *28*, 1516–1524. [[CrossRef](#)]
2. Divan, D.; Johal, H. A new concept for realizing grid power flow control. *IEEE Trans. Power Electron.* **2007**, *22*, 2253–2260. [[CrossRef](#)]
3. Xiong, L.; Zhuo, F.; Wang, F.; Liu, X.; Chen, Y.; Zhu, M.; Yi, H. Static Synchronous Generator Model: A New Perspective to Investigate Dynamic Characteristics and Stability Issues of Grid-Tied PWM Inverter. *IEEE Trans. Power Electron.* **2016**, *31*, 6264–6280. [[CrossRef](#)]
4. Thacker, T.; Boroyevich, D.; Burgos, R.; Wang, F. Phase-Locked Loop Noise Reduction via Phase Detector Implementation for Single-Phase Systems. *IEEE Trans. Ind. Electron.* **2011**, *58*, 2482–2490. [[CrossRef](#)]
5. Xiong, L.; Zhuo, F.; Wang, F.; Liu, X.; Zhu, M. A Fast Orthogonal Signal-Generation Algorithm Characterized by Noise Immunity and High Accuracy for Single-Phase Grid. *IEEE Trans. Power Electron.* **2016**, *31*, 1847–1851. [[CrossRef](#)]
6. Freijedo, F.D.; Doval-Gandoy, J.; López, Ó.; Acha, E. A generic open-loop algorithm for three-phase grid voltage/current synchronization with particular reference to phase, frequency and amplitude estimation. *IEEE Trans. Power Electron.* **2009**, *1*, 94–107. [[CrossRef](#)]
7. Lee, K.J.; Lee, J.P.; Shin, D.; Yoo, D.W.; Kim, H.J. A novel grid synchronization PLL scheme based on adaptive low-pass notch filter for grid-connected PCS. *IEEE Trans. Ind. Electron.* **2014**, *61*, 292–300. [[CrossRef](#)]
8. Mojiri, M.; Bakhshai, A.R. An adaptive notch filter for frequency estimation of a periodic signal. *IEEE Trans. Autom. Control* **2004**, *49*, 314–318. [[CrossRef](#)]
9. Lai, X.; Pei, Y.; Xiong, L. A fast Open-loop Phase Locking scheme for single-phase power grid. In Proceedings of the 2016 IEEE 8th International Power Electronics and Motion Control Conference (IPEMC-ECCE Asia), Hefei, China, 22–26 May 2016; pp. 1274–1279.
10. Xiong, L.; Zhuo, F.; Wang, F.; Liu, X.; Zhu, M.; Yi, H. A novel fast open-loop phase locking scheme based on synchronous reference frame for three-phase non-ideal power grids. *J. Power Electron.* **2016**, *16*, 1513–1525. [[CrossRef](#)]
11. Du, L.; Li, M.; Tang, Z.; Xiong, L.; Ma, X.; Tang, G. A fast positive sequence components extraction method with noise immunity in unbalanced grids. *IEEE Trans. Power Electron.* **2019**. [[CrossRef](#)]
12. Luo, A.; Chen, Y.; Shuai, Z.; Tu, C. An Improved Reactive Current Detection and Power Control Method for Single-Phase Photovoltaic Grid-Connected DG System. *IEEE Trans. Energy Conv.* **2013**, *28*, 823–831. [[CrossRef](#)]

